Project:

HyperOLED

(Grant Agreement number 732013)

"Development of high-performance, hyperfluorescence OLEDs for use in display applications and solid state lighting"

Funding Scheme: Research and Innovation Action

Call: ICT-02-2016 "Thin, Organic and Large Area Electronics"

Date of the latest version of ANNEX I: 12/10/2016

D4.4 Simulation Model for Energy Transfer

Project Coordinator (PC):	Dr. Christof PFLUMM Merck Kommandit Gesellschaft auf Aktien
Project website address:	www.hyperoled.eu
Lead Partner for Deliverable:	Fraunhofer IOF
Report Issue Date:	16/03/2020

Document History (Revisions – Amendments)	
Version and date	**Changes**
1.0 – 11/01/2020	Preliminary version & document set-up
1.1 – 08/02/2020	Description of excitation theory & Förster transfer background
1.2 – 16/03/2020	Final version

Dissemination Level		
PU	Public	**X**
PP	Restricted to other program participants (including the EC Services)	
RE	Restricted to a group specified by the consortium (including the EC Services)	
CO	Confidential, only for members of the consortium (including the EC)	

The H2020 HyperOLED project is a three-year EC funded project entitled “Development of high-performance, hyperfluorescence OLEDs for use in display applications and solid state lighting”. The project will run from January 2017 to December 2019.

The overall goal of the HyperOLED project is to develop materials and matching device architectures for high performance, hyperfluorescence organic light emitting diodes (OLEDs) for use in display applications and solid state lighting. The innovative OLEDs will be realised by combining thermally activated delayed fluorescence (TADF) molecular hosts with novel shielded fluorescence emitters, targeting saturated blue emission of very high efficiency, especially at high-brightness levels.

Further efficiency gains will be achieved through molecular alignment to enhance light outcoupling from the hyperfluorescence OLEDs. Using shielded emitters will enable simpler device structures to be used, keeping drive voltages low to be compatible with low voltage CMOS backplane electronics. This will enable demonstration of the concept’s feasibility for high-brightness, full-colour OLED microdisplays as one application example.

To develop the hyperfluorescence OLEDs, the following scientific and technical objectives will be targeted:

- Objective 1: Develop shielded emitters
- Objective 2: Develop TADF hosts
- Objective 3: Photo-physically characterise the shielded emitters and TADF hosts
- Objective 4: Anisotropic molecular orientation for enhanced performance
- Objective 5: Design and test prototype hyperfluorescence OLEDs
- Objective 6: Fabricate and evaluate demonstration hyperfluorescence microdisplays

To show the project’s overall goal has been achieved, multiple blue and white stack unit prototypes (2 x 2 mm² on 30x30mm glass substrates with ITO) will be integrated into a high-brightness microdisplay demonstrator (based on MICROOLED’s 0.38’’ WVGA CMOS backplane) and tested that demonstrate significant improvements in functionality, performance, manufacturability and reliability.

Table of Contents

1 Introduction

Emitter orientation is one parameter for optimizing the external OLED efficiency and brightness, because different emitter orientations suffer from different losses and feature different preferred emission directions. Therefore, analysing the orientation distribution of any emitting molecular ensemble is a prerequisite for an optimization of the emitting molecules as well as their hosts.

The impact of molecular orientation is expected to be apparent in the context of hyperfluorescence. This emission scheme exploits the conversion of triplet states, which are not emitting in fluorescent molecules, into singlet ones. Therefore, the donor molecule should perform TADF (thermally activated delayed fluorescence). In conclusion, the efficiency limit of 25% for fluorescence can be pushed towards 100%, because all molecular excitation can decay radiatively.

Still, the fluorophore's orientation (as acceptor of the energy transfer) remains target of optimization in order to achieve optimum outcoupling efficiency from the high index organic thin film layers, similarly to any standard device optimization. Additionally, the donor – fluorophore energy transfer, which is considered to be of Förster type, depends on the relative orientation of the donor's emissive and the fluorophore's absorptive transition dipole moments. So the detailed knowledge of molecular orientation distribution(s) is required in order to achieve a correct modelling of the hyperfluorescence energy transfer as well as an optimized outcoupling based on the fluorophore's orientation.

Any reasonable modelling of the emission layer requires data on the materials and the thin films constituting the emissive system. Especially with regard to an alignment of the emitter, material properties play an essential role. According to results from other work packages of the HyperOLED project, birefringence of the host material and emitter orientation can both explain emission patterns of anisotropic ensembles. However, the separation of both effects is possible and necessary when attempting to understand the processes arising in emissive layers.

Here, we assume that such data is available, i.e., that both the orientation distribution of the emitters as well as the anisotropy of the materials involved is known. With such basis, the available description of the emitter's radiation has been shown to be a valid starting point for any simulations containing additional effects, such as fluorescence resonant energy transfer.

This document gives a representative overview on the approaches conducted for simulating energy transfer effects electro-dynamically. Therefore, the excitation and emission of a single molecule is discussed first in section 2, which is followed by the description of inter-molecular effects (energy transfer) in section 3. An approach to describe the emission of a whole molecular ensemble, as relevant for active devices like OLED, concludes this document.

2 Excitation and intra-molecular effects

2.1 Introductory remarks

In an OLED, excited states are generated by the recombination of charge carriers that causes an excited molecular state. Such a process is commonly assumed to be isotropic, i.e., it does not excite any molecular orientation preferably. In contrast, any optical excitation relies on electromagnetic fields, which are characterized by a propagation direction and a polarization. The latter being defined as the oscillation direction of the electric field. Even for the non-propagating near fields of a source, there is a distinct orientation relation between donor and acceptor, which introduces two angles of orientation (that of the donor and that of the acceptor relative to the separation vector between both).

As a very first approach to this issue one needs to tackle the excitation of a single emitter by a polarized electromagnetic wave. Such case can be generated by exciting any luminescing sample with a laser beam. This experiment is continuously done in the optical analysis of emitter orientation. Therefore the first chapter describes the theoretical background and the theoretical approach for modelling the emission of optically excited molecular ensembles. It is the starting point for analysing the connection between excitation and emission directions in molecular ensembles and must be considered in any energy transfer simulations as well.

2.2 Theoretical model

2.2.1 Emission pattern model

The intensity emission pattern generated in the far-field by a single oscillating (point) dipole $\vec{p}_{em}$ is modelled according to the equation

$$I_{far}^{single}(\theta, \lambda, pol) \sim \frac{I_{stat}(\vec{p}_{em}, \lambda)}{\Gamma(\vec{p}_{em}, q)}$$

with emission wavelength λ, intrinsic quantum efficiency q, polarization indicated by “pol” and emission rate Γ. The latter includes emission rate variations due to the optical environment (i.e. interfaces or micro cavities) and is well-known as Purcell effect. The stationary emission pattern I_{stat} is that of a single, continuously pumped source well-known from text books as Hertz dipole. Note, that this stationary pattern I_{stat} readily contains all interference effects but misses the Purcell effect.

Extending this description to emitting layers, which contain multiple sources, requires one to sum or to average this intensity pattern over all emitters at all positions z along the layer’s height. Indicating this average by brackets yields formally

$$I_{far}(\theta, \lambda, pol) \sim \left\langle w(z) \cdot \frac{I_{stat}(\vec{p}_{em}, \lambda, z)}{\Gamma(\vec{p}_{em}, q, z)} \right\rangle_{z, \vec{p}_{em}} ,$$

i.e., the emission patterns of all emitters (single molecules) are summed or averaged with a weighting function w(z). This weighting function can consider any spatial distribution of the rate of light generation and is referred to as the profile of the emission zone in an OLED. For optical excitation, it is associated with the spatial distribution of the excitation intensity due to interference effects within the emitting layer.

2.2.2 Excitation models

The excitation rate will depend on the mutual orientation between the electric field $\vec{E}$ and the (absorbing) dipole $\vec{p}_{abs}$. With regard to previous investigations, and especially to the experimental analysis of materials and orientations, it is worth noting that two different approaches can be conducted for modelling such an excitation:

The first approach is based on the absorption dipole moment, yielding

$$w_p(z) \sim [\vec{p}_{\mathrm{abs}}, \vec{p}^{*}_{abs}] \cdot \vec{E}(\mathrm{z}) \cdot \vec{E}^{*}(z)$$

the product of the intensity distribution *EE** with the dyadic product of the absorption dipole moment. So the alignment of the emitters is introduced by the orientation of their transition dipole moments, which needs to be averaged over the ensemble. Alternatively, one might describe the excitation via the absorption (imaginary part of the permittivity tensor ε) of the material according to

$$w_\varepsilon(z) \sim \mathrm{Im}[\hat{\varepsilon}\vec{E}(\mathrm{z}) \cdot \vec{E}^{*}(z)] \quad .$$

Whilst the first approach relies on a single molecule description, the second one readily contains the ensemble average of the absorbing transition dipoles.

Practically, the measurement of the orientation distribution of $\vec{p}_{abs}$ is achieved by estimating the orientation distribution of the emission transition dipole moments $\vec{p}_{em}$. Both quantities might differ, as dye molecules are known to potentially exhibit an angle between excitation and emission moments. Alternatively, the measurement of the permittivity tensor suffers from a limited accuracy usually, which prevents extracting orientation data of co-doped emitters in the relevant concentration range below 20%. These considerations led to the characterization efforts spent in the previous tasks of the project and illustrate the importance of consistent characterization tools.

2.3 Intra-molecular effects

Organic molecules might exhibit an angle Ω between absorption and emission transition dipoles, as sketched in Figure 2.1 below. As there is a priori no preferred direction into which the emission transition dipole is tilted, we assume that the emission originates equally distributed from a cone around the absorption transition dipole. This is modelled by assuming a constant distribution along the rotation angle χ.

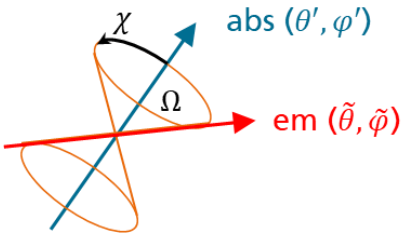

Figure 2.1: Sketch of the emitter geometry and the angle between absorbing (blue) and emitting (red) transition dipole moments spanning a cone with angle Ω.

Introducing such model on the relative orientation of transition moments in the emitting molecule(s) requires to model the orientation distribution of the molecular ensemble via the distribution of its absorption transition moments. This differs from the approach commonly conducted in OLED material physics, where the orientation of emitting transition moments is specified.

As detailed above, the emission pattern in an OLED originates from an isotropic excitation of the emitters, thus exhibiting a cylindrical symmetry. But, when the excitation is achieved with a linearly polarized laser, the cylindrical symmetry is lost due to the oriented excitation. Such effect is exploited in physical chemistry, where the depolarization of fluorescence emission is measured in order to analyze e.g. rotational diffusion of emitting molecules.

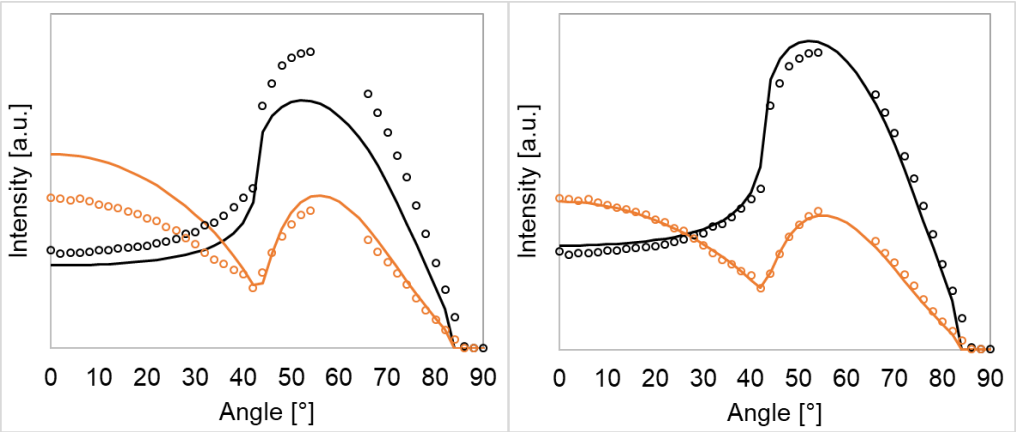

Figure 2.2: Emission pattern measurements (dots) of a ~30 nm thin film on a fused silica substrate for TE (black) and TM (orange) polarization plotted with the fitted distributions (lines) when assuming no angle (Ω=0 left) or a finite angle (right) between absorption and emission transition dipoles.

Figure 2.2 illustrates the effect on the basis of a thin film's photoluminescence emission pattern inside the substrate. Without assuming an angle between absorption and emission dipoles, a bad fit is obtained only; the discrepancies cannot be removed by varying the emitter orientation. But when including such a difference between absorption and emission directions in the emitting molecule, a proper fit can be reached. However, note that additional effects outlined below might also affect the output of such experiment.

3 Energy transfer and inter-molecular effects

3.1 General context

The fluorescence resonance energy transfer (FRET), a radiation-less energy transfer from a donor (D) to an acceptor (A), is important in many different applications scenarios, as e.g. for proteins in photosynthesis or for adjacent nanoparticles. It describes the non-radiative interaction of two molecules, one donor and one acceptor of the energy.

Initially, the donor (D) is brought to an excited state (excitation energy ~ω_D), while the acceptor (A) is still in its ground state. The excitation of the acceptor (excitation energy: ~ω_A < ~ω_D) is described by a transfer rate $\Gamma_{D\to A}$ (see Figure 3.1a, b). It depends strongly on

(i) The overlap of the donor's emission spectrum $f_D(\omega)$ and the acceptor's absorption spectrum $\alpha_A(\omega)$
(ii) the distance r between donor and acceptor
(iii) the orientation of the donor ($\vec{p}_D = p_D\vec{n}_D$) and acceptor dipole moments ($\vec{p}_A = p_A\vec{n}_A$) with respect to the donor-acceptor-distance vector ($\vec{r} = r\vec{n}_r$) .

Here, the orientation vectors ($\vec{n}_A, \vec{n}_D, \vec{n}_r$) are unit vectors, where each of them is governed by an individual, statistical distribution function. Usually, FRET is considered in a homogeneous, isotropic environment described by an isotropic dielectric function ε or refractive index $\varepsilon = n^2$. But, as outlined above, the HyperOLED project utilizes FRET in an anisotropic OLED layer system (see Figure 3.1a). Each optical layer is characterized by an uniaxial dielectric tensor $\hat{\varepsilon}$ with extraordinary ("perpendicular") $\varepsilon_\perp = n_\perp^2$ and an ordinary ("parallel") component $\varepsilon_{||} = n_{||}^2$. The symmetry axis (optical axis) of the tensor is parallel to the layer normal vector.

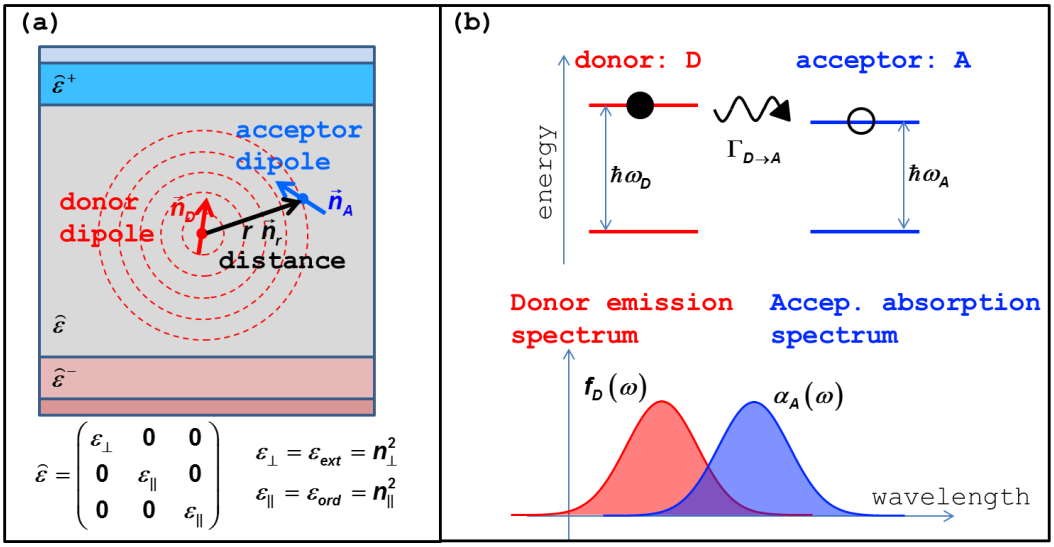

Figure 3.1: Fluorescence resonance energy transfer (FRET) in OLEDs. (a) Schematic illustration of FRET in an anisotropic OLED layer system ($\hat{\varepsilon}$: dielectric tensor of each layer, ($\vec{n}_A, \vec{n}_D, \vec{n}_r$): orientational unit vectors of the acceptor (A) and donor (D) dipole moments as well as the D-A-distance. (b) Spectral illustration of FRET as an energy transition from an excited donor state (donor energy ~ω_D) to an acceptor state (acceptor energy ~ω_A) where the transition rate $\Gamma_{D\to A}$ depends on the overlap of the donor emission spectrum ($f_D(\omega)$) with the acceptor absorption spectrum ($\alpha_A(\omega)$) as well as on the relative orientation of both transition dipoles.

Both FRET as well as spontaneous emission are quantum mechanical processes. Their main features can be described by classical electrodynamics. Within this background, decay or

transfer rates scale proportionally to the total electrodynamic power *P* transferred classically. Its power density dP/dV is determined by Poynting's theorem

$$\frac{dP}{dV} = \frac{d\ Power}{d\ Volume} = \frac{1}{2}\omega \mathrm{Im}\left[\vec{\Pi}\ \vec{E}^*\right]$$

and depends on the relevant electric field $\vec{E}$ and polarisation $\vec{\Pi}$ with the angular light frequency ω.

When calculating the spontaneous emission of a donor (D), the decay rate is proportional to the totally irradiated power due to the donor's polarisation $\vec{\Pi} \sim \overrightarrow{p_D}\delta(r - r_D)$ that originates from the donor dipole moment ($\vec{p}_D = p_D\vec{n}_D$)

$$\Gamma_{spon} \sim P_0 = \frac{1}{2}\omega \vec{p}_D \,\mathrm{Im}\left[\vec{E}_D^*\left(\vec{r}_D\right)\right] .$$

Here, the electric field as well as the polarisation originate from the same donor dipole moment $\vec{p}_D$. Thus, the imaginary part of the donor field exactly at the donor position (see red labelled symbols in above equation) enters the equation for the decay rate of spontaneous emission. Although the real part of a dipole field is singular at the donor position, the corresponding imaginary part appearing in above equation remains finite.

In order to simulate FRET, the power transferred from the donor to the acceptor has to be determined. Thus, the relevant polarisation is given by the acceptor dipole induced by the electric donor field. The induced acceptor dipole can be described by the acceptor polarizability tensor as $\vec{p}_A = \hat{\alpha}_A\vec{E}_D(\vec{r}_A) = \alpha_A^0\vec{n}_A \otimes \vec{n}_A\vec{E}_D(\vec{r}_A)$ and the transfer rate reads as

$$\Gamma_{D\to A} \sim P_{D\to A} = \frac{1}{2}\omega \mathrm{Im}\left[\alpha_A^0\right]\left|\left\langle \vec{n}_A \,|\, \vec{E}_D\left(\vec{r}_A\right)\right\rangle\right|^2 .$$

Now, the square of the absolute amount (real and imaginary part) of the donor field at the acceptor position (see blue symbol) determines the transfer rate. Thus, for decreasing donor-acceptor distances the FRET rate increases considerably due to the dipole near fields. For OLED simulation one has to tackle both the radiative far field effects but also the divergent near fields.

3.2 Field structure

In order to access the spatial distribution of energy transfer, the field distribution inside the stack needs to be modelled. This has been achieved by means of an existing implementation of the Green's function formalism called "Radiating Slabs". Originally implemented to simulate emission patterns and the Purcell effect, this formalism had been extended to calculate the full electromagnetic fields inside a stratified system based on the Green's function $\hat{G}$. For a donor dipole $\vec{p}(\vec{r}_D)$ the electric field $\vec{E}$ at any acceptor position $\vec{r}_A$ is given by the equation

$$\vec{E}_D(\vec{r}_A) = \omega^2\mu_0 \cdot \hat{G}(\vec{r}_A, \vec{r}_D) \cdot \vec{p}(\vec{r}_D) \quad ,$$

where $\hat{G}$ is expended into plane waves. These plane waves are called the "modes" of the system. Each mode is defined by its propagation constant $k_{||}$ (sometime called in-plane wave vector). In general, $0 \le k_{||} < \infty$ need to be considered.

For emission into the far-field, only small propagation constants $k_{||} < k_{limit}$ contribute to the emission pattern. Small values $k_{||} < 1$ are proportional to the sine of the emission angle in air. Concerning propagation inside the stack of high refractive layers, the value of k_{limit} depends on the system under consideration and is associated with the material exhibiting the highest refractive index in most cases. Much larger values of $k_{||}$ describe so-called evanescent modes

inside the system and can be associated with near field components of the donor. Utilizing such discrimination of near-fields (large $k_{||}$) and propagating (small $k_{||}$) fields allows to sketch the spatial distribution of dipole fields inside a layered system (Figure 3.2).

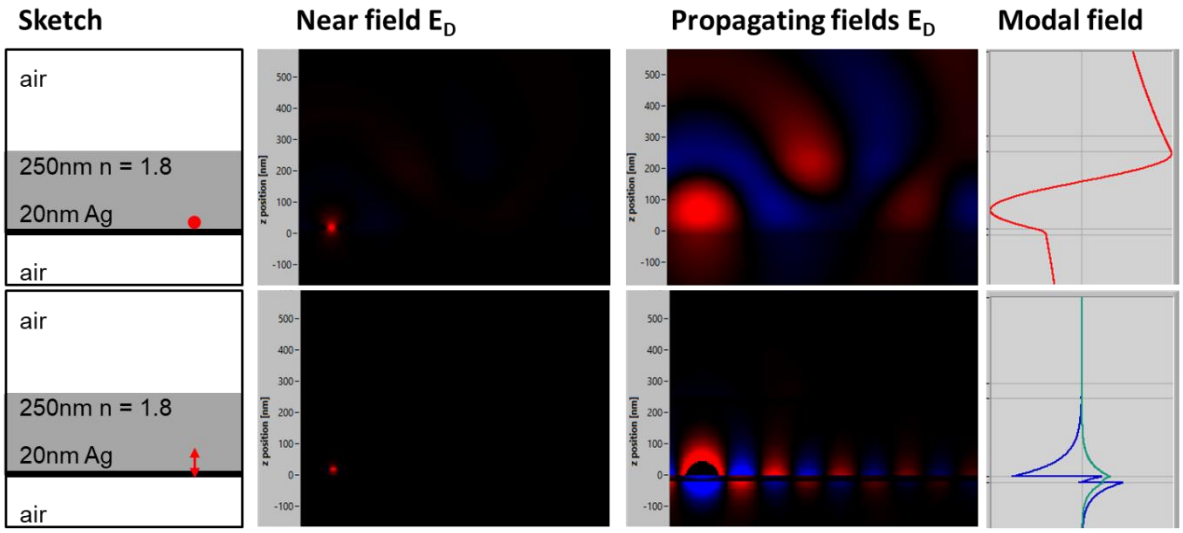

Figure 3.2: Distribution of the emitter's electric field for a parallel (top, parallel electric field component) and a perpendicular (bottom, perpendicular component of the electric field) emitter inside a 250 nm thick layer with refractive index n=1.80 surrounded by one 20 nm thin Silver layer (one side) and air (both sides). The images sketch the situation (left column), plot the near field and propagating field components (middle columns) as well as the field structure of the major excited mode (right column, electric field components of the TE (top) and TM (bottom) modes are plotted).

For the situation of an emitter close to a metal as chosen in Figure 3.2, a parallel or perpendicularly oriented emitter excites a transvers electrically polarized ("TE") or a transvers magnetically polarized mode ("TM"), respectively. Note, that the latter corresponds to exciting a surface plasmon – polariton, which can be a major channel of optical losses in standard OLED structures. Both modes propagate along the structure and could potentially excite acceptors on micrometer length scales. Contrarily, the donor's near-field is solely limited to the vicinity of the emitter in the 1…10 nm range and seems not to be disturbed by the layered system in the plot above.

However, the propagating fields exhibit a $1/r_{D\to A}^{1}$ distance dependence, while near field components in order of $1/r_{D\to A}^{3}$ appear. Therefore, near-fields dominate the energy transfer in the small distance range. With regard to the effect of the layered system on such energy transfer, we recall that only very large values of $k_{||}$ contribute to the near fields, so only nearby interfaces might modify such transfer rates and will be discussed in the next paragraph.

3.3 Interface effect on FRET

Obviously, the above mentioned field distributions can be modelled rigorously in order to determine the donor's field at the acceptor's position. But, such approach requires significant calculation efforts and shall thus be simplified in order to speed up simulation. Therefore, a classical analog has been used and is illustrated in Figure 3.3.

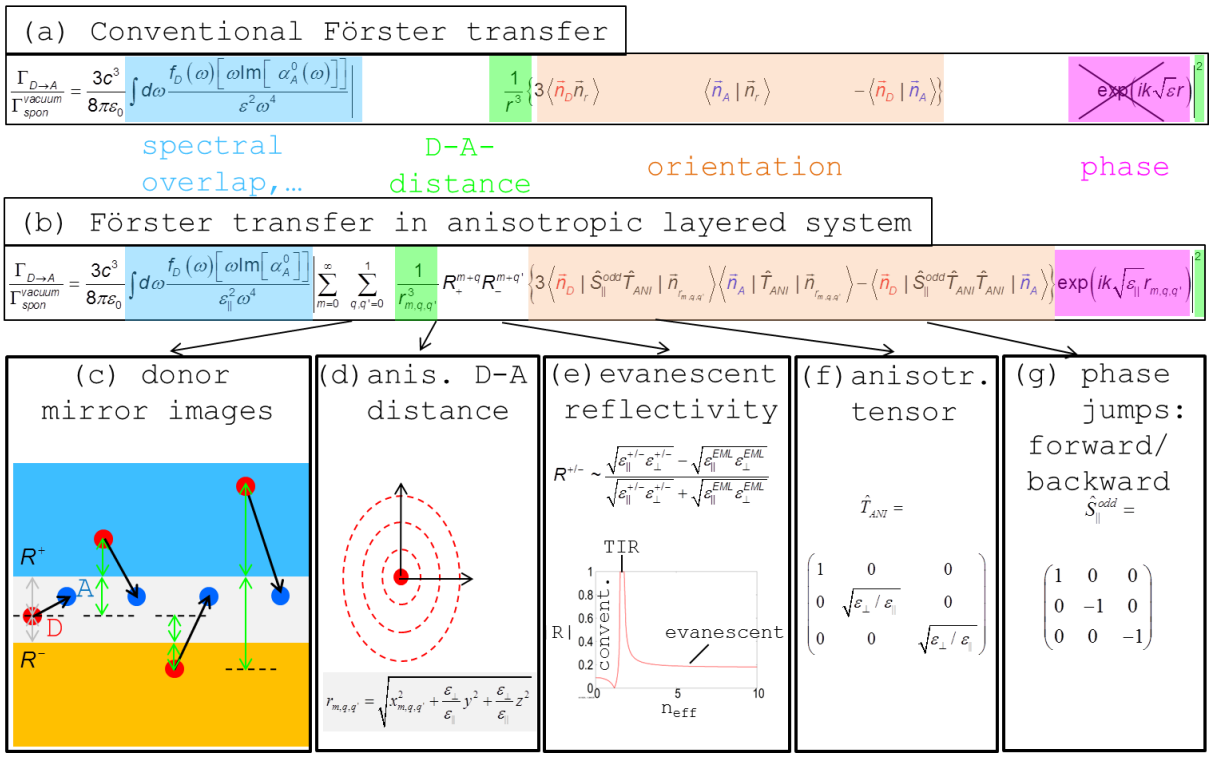

Figure 3.3: Comparison of the Förster transfer rate for isotropic, homogeneous media (a) with the one in anisotropic layered systems (b). The formal description is qualitatively similar as illustrated by the shaded terms in (a) and (b) using the colours blue – spectral donor-acceptor overlap, green – distance dependency, orange – orientation dependency, magenta – phase accumulation.
(c – g) illustrate differences of both models: (c) Starting from the original donor (most left red sphere), additional donor mirror images (additional red spheres) with varying distance vectors (black arrows) have to be considered. (d) The anisotropy of the EML leads to an effective scaling of the spatial coordinates. (e) The evanescent reflectivities of the lower/upper stack serve as the mirror image amplitudes; here only simple Fresnel coefficients are shown. (f) The EML anisotropy leads to an effectively different dipole moment strength considered by the anisotropy tensor. (g) The forwardly and backwardly emitted transverse dipole fields possess an π phase difference for odd mirror image indexes considered by the operator $\hat{S}_{||}^{odd}$.

Förster transfer effects in a thin layer are formally compared with the well-known energy transfer in a homogeneous medium. Summarizing shortly, the presence of the interfaces generates image donors. Then, all donor images can transfer energy onto the acceptor. Fortunately, this theoretically infinite series of donor images can be truncated after a few terms: An increasing number of donor reflections corresponds with an increasing distance of the donor image to the acceptor. So the $1/r^6$ distance dependence of the energy transfer (compare Figure 3.3c) allows to take the first few terms into account only: Practically, keeping layer thicknesses in the order of ~10 nm in Organic LED in mind, a single donor image at one nearby interface remains as the most pronounced effect of the thin film system only.

Furthermore, because near fields that exhibit large propagation constants are considered only, the reflectivity of the fields at the interfaces can be approximated by a constant with respect to $k_{||}$ -variations (Figure 3.3e). Obviously, also the anisotropy of the background (Figure 3.3d) and the phase jumps of the fields at the donor's position need to be considered (Figure 3.3f).

This analytical model covers all aspects associated with the energy transfer from a donor dipole onto an acceptor dipole in a system of uniaxially birefringent layers. Utilizing this model enables to compare the energy transfer in a layered thin film system with that in homogeneous media. Concluding shortly, the major changes arise from

(i) some different scaling with ordinary and extraordinary indexes due to anisotropy of the materials, and
(ii) the appearance of donor mirror images due to the upper and the lower stack's evanescent reflectivities, which lead to a sum of interference terms.

As the Förster transfer is dominated by effects in the vicinity of the donor, only the anisotropies in the active layer or nearby layers/interfaces need to be considered.

4 Description of the emitting ensemble

4.1 Introduction

All discussion above relates to a single emitting dipole (section 2) or to the energy transfer of one donor onto one acceptor (section 3). Now, this treatment needs to be extended to model the emission of the whole ensemble of emitters inside the emitting layer, when this layer is embedded inside a potentially thin film stack. Obviously, all effects discussed so far need to be considered.

4.2 Theoretical Description

As outlined above, the energy transfer (Förster transfer) requires modelling the donor molecule's field at the position of the acceptor. As the donor's fields can be described analytically, an analytical implementation of the effects can be sought, e.g. by exploiting the Green's function approach mentioned in section 3.2. But, such an analytical approach requires integrating all distributions involved, which consist of three spatial (the distribution of molecules in the active layer), two angles representing the orientation of each molecule, as well as the orientation of the emitting relative to the absorbing transition dipole moment (i.e. the exact location on the cone spanned by the angle Ω). In conclusion, no analytical integration of all these distributions has been found.

Instead, the emission of an ensemble of emitters can be described by the rate equation of a single emitter, taking the interactions between the emitters (Förster transfer) into account. This yields a rate equation for the emitting ensemble:

$$\partial_t N_i = -\left[\Gamma_{nr} + \Gamma_{rad}^{(i)} + \sum_{k\neq i}\Gamma_T\left(r_{i,rad} \rightarrow r_{k,abs}\right)\right]N_i + \sum_{k\neq i}\Gamma_T\left(r_{k,rad} \rightarrow r_{i,abs}\right)N_k + W_{i,abs}$$

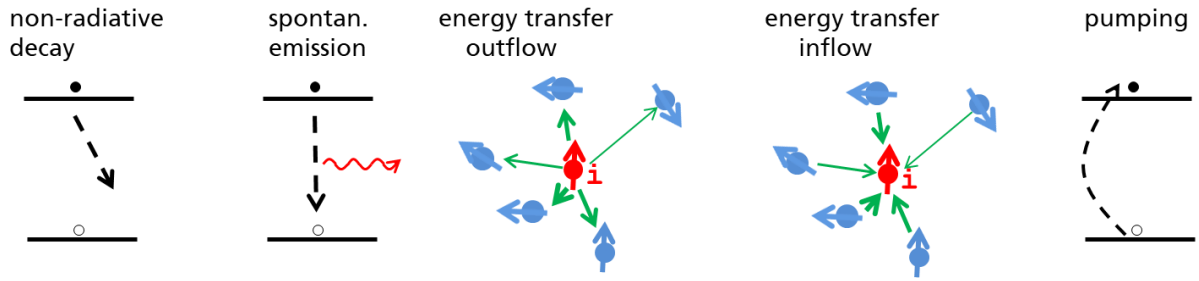

Figure 4.1: Visualization of the different terms in the rate equation of emitter i.

In this equation the population N_i of molecule's *i* excited state is described. It is reduced by non-radiative and radiative decay (Γ_{nr} + Γ_{rad}) as well as by energy transfer to another molecule ($\Gamma_T(r_i \rightarrow r_k)$). In contrast, the excitation of i is increased by energy transfer from another molecule ($\Gamma_T(r_k \rightarrow r_i)$) as well as by any other excitation $W_{i,abs}$ (e.g. electrical or optical pumping).

Two issues are worth to note explicitly with regard to this rate equation:

(i) The rate equation is considered in the small excitation limit, i.e. potential saturation effects of the emitter's excitation are not taken into account. It applies to typical OLED related situations very well.

(ii) Regarding the energy transfer $r_i \rightarrow r_k$ and $r_k \rightarrow r_i$ the approach is symmetric. However, keeping in mind any deviation of absorbing and emitting transition dipoles in real molecules removes this symmetry. So for cases in which both transition moments

differ, depopulation (~N_i) and population (~N_k) terms are not symmetric any more. This points out the necessity to include the angle Ω in the modelling.

This description is the general case of a luminescing molecular ensemble. It contains the well-known Purcell effect that enters e.g. via a position dependent spontaneous emission rate Γ_{rad} as well as orientation dependent Förster Γ_T and emission rates $\Gamma_{rad.}$ Therefore, cavity effects enter all terms (spontaneous emission, energy transfer, pumping) except the non-radiative deactivation, which is assumed to be a material property and not to be modified by optical processes.

4.3 Orientation averaging models

It is worth pointing out that two different limiting cases can be deduced from this description. In the first case, the energy transfer is small ($\Gamma_{nr} + \Gamma_{rad} \gg \Gamma_T$), thus removing all coupling of neighboring emitters. Then, each emitter is described by the well-known rate equation

$$\delta N_i = -[\Gamma_{nr} + \Gamma_{rad}^i] \cdot N_i + W_{i,abs} \quad .$$

In conclusion, the temporal emission is solely described by the non-radiative and radiative (incl. Purcell effects) depopulation of the excited state, and a single exponential temporal decay according to the emitter orientation near an interface will be observed experimentally.

The contrary case is the one with pronounced coupling $\Gamma_{nr} + \Gamma_{rad} \sim \Gamma_T$ of neighboring emitters and yields two major conclusions: First, a single excited emitter experiences additional decay channels, as energy can be transferred to the neighbors. Thus, the total rate of depopulation increases and the lifetime decreases. Second, the sum of energy exchange rates can exceed the emission rate. Then, individual molecules become indistinguishable in the emission and ensembles with averaged properties can be observed only. Such properties include e.g. the emission lifetime, which is averaged over all orientations.

It is worth to note that the energy transfer can be adjusted by the intermolecular distance. Therefore, the related effects shall become accessible experimentally when varying molecular concentration(s). One example is summarized for illustration purposes below.

4.4 Example

The approach described above has been implemented for simulation purposes. Utilizing a Monte Carlo representation of the emitter ensemble allows for solving the rate equation of the ensemble while considering all relevant effects outlined above. In order to illustrate the effect, an example comparable to the one introduced in section 2 is plotted in Figure 4.2.

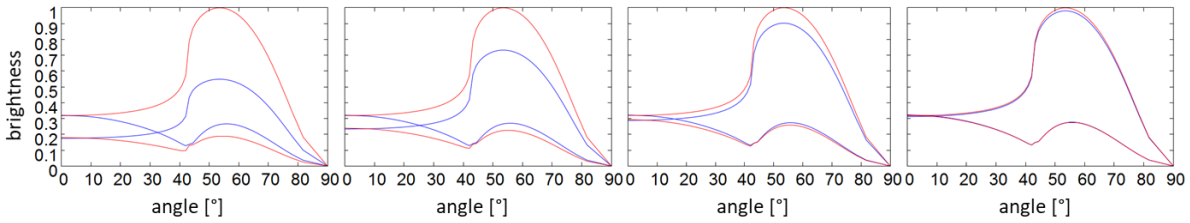

Figure 4.2: Emission patterns (compare Figure 2.2) for two different geometries of optical excitation (plotted as red / blue graphs) and assuming a different amount of inter-molecular energy transfer from very low (left) to very large (right).

Apparently, in the case of rather small energy transfer, different excitation orientations yield different emission patterns (left diagram). This appears due to the photoselection imposed by the polarization of the excitation (laser) beam. This causes e.g. the perpendicularly emitted intensities to depend on the excitation polarization, as apparent by the splitting of the intensities at 0°. Increasing the energy transfer decreases differences in the emission patterns, i.e. the patterns plotted in blue and in red converge. In such case, photoselection due to the excitation is still present. But, as explained in section 3, the energy transfer based coupling between the emitters removes such anisotropy from the emission pattern.

5 Summary and Conclusions

The HyperOLED project addresses energy transfer effects in planar, layered structures. Therefore, anisotropic optical effects arising due to anisotropic materials as well as aligned emitters need to be described for simulation, characterization and optimization purposes. Additionally, fluorescence resonance energy transfer within such systems has to be taken into account.

A simulation model has been developed for this reason; accompanying experiments have been performed in parallel and will be reported separately. According to these results, the effects of

- anisotropic material dispersion (uniaxial model)
- donor / acceptor orientation distribution
- angle between the acceptors absorption and transition dipole moments
- different kinds of emitter excitation (electrical pumping, optical pumping including photoselection and interference)
- finite intrinsic quantum efficiency including the impact of the optical cavity (Purcell effect)
- near-field energy transfer based on analytical approximation

are included in the simulation model, which combines multiple anisotropic effects. The implementation utilizes a Monte Carlo representation of the emitting ensemble, thus enabling to simulate emission properties of different types of molecular ensembles.

Obviously, energy transfer is linked to emitter orientation effects, which are desired to enhance the external efficiency of active devices via improved outcoupling. So the major aspects considered are directly related to orientation effects. In detail, the ensembles behavior upon optical excitation, which has become the standard method of emitter characterization, has been analyzed in detail and yields the following conclusions.

First, two different ensemble averages are qualitatively predicted. One limit is the case of low coupling, exhibiting the single emitter's properties in the emission pattern. The other limit is the case of strong near-field coupling. In such case, energy exchange between emitters is faster than the emission process. This leads to a situation in which no single emitter property is observable anymore; the far-field emission is that of an ensemble-averaged emitter. As this behavior modifies the emitter's properties, it needs to be considered thoroughly for all characterization and simulation efforts.

Second, and probably even more important, the latter limit seems to apply to practically all emitting systems in Organic LED, indicating energy transfer to govern the emitter properties. This points out the importance of energy transfer for the molecular picture of the light emission process, and potentially indicates new approaches for characterizing molecular systems.